ELSEVIER

Journal of Photochemistry and Photobiology A: Chemistry 112 (1998) 239–244

Journal of Photochemistry and Photobiology A:Chemistry

Photochemical property and surface characterization of silver-loaded zirconium phosphate

Hirokazu Miyoshi [a,*], Masamitsu Ieyasu [b], Tomio Yoshino [a], Hiroki Kourai [b]

[a] *Department of Radiological Technology, School of Medical Sciences, The University of Tokushima, 3-18-15 Kuramoto-cho, Tokushima 770, Japan*

[b] *Department of Bioscience and Technology, Faculty of Engineering, The University of Tokushima, 2-1 Minamijousanjima-cho, Tokushima 770, Japan*

Accepted 9 October 1997

Abstract

Superoxide radicals such as $OH^{\cdot}$ and $O_2^{-\cdot}$ were detected by DMPO as a spin trap reagent in visible light-irradiated silver-loaded zirconium phosphate [$Ag_{1-x}H_xZr_2(PO_4)_3$] water suspension. It depended on Ag content and irradiation wavelength. When no-silver-loaded zirconium phosphate [$HZr_2(PO_4)_3$]/Nafion-modified Pt electrode in 0.1 mol dm^{-3} Na_2SO_4 aqueous solution was irradiated with 500 W superhigh pressure mercury lamp, a 26.1 $\mu A\ cm^{-2}$ photocathodic current was observed at -0.2 V vs. SCE. This indicated that the formation of superoxides was due to the charge separation on the photoirradiated $HZr_2(PO_4)_3$. In the loading of Ag^+ ions to the zirconium phosphate, it was found that Ag^+ ions were mostly located on the surface and were stabilized by the surrounded oxygen atoms. Furthermore, Raman shifts due to an interaction between O_2 and Ag for $Ag_{1-x}H_xZr_2(PO_4)_3$ were observed by FT-Raman technique. The ESR peak at $g=2.0036$ was detected in vacuo and in the air it was disappeared. This g value was similar to that which is due to the conduction electron in small silver nanocrystallites. Such conduction electron in $Ag_{1-x}H_xZr_2(PO_4)_3$ seemed to be due to the increase of the electron density of Ag^+ by the effects of the octahedrally surrounded oxygen such as $-I$ effects. It was found that the Ag^+ site worked as an electron pool. Consequently, it was suggested that photogenerated electron reduced O_2 to O_2^- radical via the $Ag_{surface}{}^+$ site and the remaining hole on the zirconium phosphate oxidized OH^- in the aqueous solution to OH radical.

Keywords: Superoxide radicals; Ag; Zirconium phosphate; Spin-trap method; Raman spectra; Charge separation

1. Introduction

A lot of studies on preparations and photochemical properties of silver clusters have been reported for a decade. In 1979 and 1981 Henglein had reported that colloidal silver was prepared in an aqueous solution by radiolysis of water and H_2 evolution from water by injection of electron to colloidal silver [1,2]. Sun and Seff [3] reviewed a structure of Ag cluster prepared in zeolite by using FT-IR and ESR methods and the photocatalytic property of Ag cluster in zeolite. Recently, Michalik et al. [4] reported that in synthetic clay a silver cluster was prepared and the ESR spectra were showed. Thus silver clusters prepared in the above methods were tried to use as catalyst. For example, Ag cluster dispersed on SiO_2 was used in the selective oxidation of ethylene to ethylene oxide [5]. Specially, as the photocatalyst it was reported that Cl^- ion oxidized to Cl_2 by self-sensitization of Ag^+ to/from Ag^0 in Ag cluster in zeolite under light irradiation [3]. On the other hand, in 1996 the photocatalytic property of Ag^+ ion was reported by Matsuoka et al., that is, the photocatalytic decomposition of nitric oxide on Ag^+ ion-exchanged zeolite by excitation of the Ag^+ ion, not the Ag cluster [6]. Furthermore, Kourai et. al. has reported that silver zirconium phosphate [$Ag_xH_{1-x}Zr_2(PO_4)_3$] powder acted as an antibacterial agent for *Escherichia coli* K12 W3110 in water suspension under visible light irradiation for 30 min at 303 K [7,8]. It was prepared by ion-exchange of Ag^+ ion with H^+ ion in $HZr_2(PO_4)_3$, which had three-dimensional skeletal structure composed of ZrO_6 and PO_4 [9]. An interspace of it forms a tunnel structure. After Ag^+ ion was loaded to $HZr_2(PO_4)_3$ to be 3.7, 7 or 11 wt.%, Ag^+ ion-exchanged zirconium phosphate was heated at 1473 K in the air and a white powder of cubic crystal (0.3–0.5 μm) was obtained [7,8]. This antibacterial property depended on the Ag content and seemed to be due to superoxide radicals generated by light irradiation. However, the mechanism of photogeneration for superoxide radicals on the agent and the role of the Ag^+ ion is not clear.

In this study to detect superoxide radicals, ESR technique with spin-trap reagent 5,5-dimethyl-pyrrolidine-*N*-oxide

* Corresponding author. Tel.: +81-886-31-3111; fax: +81-886-33-7398.

1010-6030/98/$19.00
PII S1010-6030(97)00286-4

(DMPO) was applied. And the generation mechanism of superoxide radicals on irradiated $Ag_xH_{1-x}Zr_2(PO_4)_3$ powder was discussed with the surface analysis methods of XPS and FT-Raman and ESR technique.

2. Experimental details

2.1. Chemicals

Three kinds of $Ag_xH_{1-x}Zr_2(PO_4)_3$ (3.7 wt.%, 7 wt.%, 11 wt.% Ag content), $NH_4Zr_2(PO_4)_3$, and $HZr_2(PO_4)_3$ powders were provided by Toa Gousei, 5,5-dimethyl-pyrrolidine-*N*-oxide (DMPO, LC-9130), 2,2,6,6-tetramethyl-1-piperidine-*N*-oxyl nitroxide (TEMPO), superoxide dismutase (SOD, LM-9504)) were obtained from Labotec. Nafion used was Aldrich 117 Nafion (5 wt.% Nafion–alcoholic solution). These reagents have been used in our investigations directly without further purification.

2.2. ESR measurement

Measurements of ESR spectra were performed with JEOL TE-300 and ESPRIT-425 data system. Superoxide radicals were detected with the spin-trap method as follows. 5,5-dimethyl-pyrrolidine-*N*-oxide was used as a spin-trap reagent. ESR spectra (X-band) of DMPO adducts were measured with a JEOL DATUM LC12 quartz oblique cell for an aqueous solution. Concentration of DMPO-OH was determined by comparing the area of DMPO-OH for that of 3.2×10^{-6} mol dm^{-3} TEMPO aqueous solution as a standard in the respective ESR spectrum. 0.4 cm^3 or 0.2 cm^3 $Ag_xH_{1-x}Zr_2(PO_4)_3$ powder suspension (1 mg cm^{-3}) was mixed with 0.02 cm^3 DMPO spin-trapping reagent (9.0 mol dm^{-3}) and added to the cell. ESR spectra were measured during irradiation of 500 W Xe lamp (Ushio, UI-501C) at room temperature.: 8 mW power, 79 μT modulation width, Mn (II)/MgO external standard for g value, ±5 mT sweep width. Irradiation wavelength was selected to be 400 nm, 500 nm, 600 nm, and 700 nm with cut-off filters (UV-37, Y-48, O-58, Toshiba Glass) and interference filters (KL-40, 50, 60, 70, Toshiba Glass). Quantum efficiencies of the generation of DMPO-OH at 400 nm and 500 nm were determined with 0.006 mol dm^{-3} and 0.15 mol dm^{-3} of Fe^{3+}–oxalato chemical actinometries. The measurements of $Ag_xH_{1-x}Zr_2(PO_4)_3$ (3.7 wt.%, 7 wt.%, 11 wt.% Ag content), $NH_4Zr_2(PO_4)_3$, and $HZr_2(PO_4)_3$ powders were performed at room temperature, 77 K, and 423 K as follows. After 60 mg of those powders were added in the 5 mm Φ quartz tube for X-band measurement, the air in the tube was removed by using the vacuum pump for about 30 min. The degassed tube was sealed with melting glass and they were used for ESR measurements. ESR spectra at 423 K were measured during heating by the temperature control unit (JEOL, ES-DVT3). To investigate the effect of the air, ESR spectra of the samples in the air-loaded tube were measured at room temperature.

2.3. Photoelectrochemical measurement

Absorption spectra of $Ag_xH_{1-x}Zr_2(PO_4)_3$ (3.7 wt.%, 7 wt.%, 11 wt.% Ag content), $NH_4Zr_2(PO_4)_3$, and $HZr_2(PO_4)_3$ suspensions in water (0.3 mg cm^{-3}) were measured with a spectrophotometer (Hitachi, U-2000) at room temperature.

A $HZr_2(PO_4)_3$/Nafion-modified electrode was prepared by coating a Pt plate (2 cm diameter) with a 0.4 cm^3 $HZr_2(PO_4)_3$/Nafion suspension (1 mg cm^{-3}), followed by drying. A quartz cell with a flat window was used for photoelectrochemical measurements. It contained a Pt counter electrode and a saturated calomel reference electrode (SCE). For electrical measurements, a potentiostat (Hokuto Denko, HA-301), a potential sweeper (Hokuto Denko, HB104), an X-Y recorder (Yokogawa Electric Works, Model 3022), and a pen recorder (Yokogawa Electric Works, Type 3056) were used. Photocurrents were measured at -0.2 V vs. SCE during irradiation with a 500 W superhigh pressure mercury lamp (Ushio, UI-501C) through UV-35 cut-off filter.

2.4. Surface analysis

XPS spectra of them were measured with Shimadzu ESCA-1000AX. Mg-Kα (1253.6 eV) was employed as X-ray source. Data processing was carried out with HP 340. The ESCA-1000AX was operated at 10 kV and 30 mA under a pressure of 10^{-6}–10^{-7} Pa. The binding energy was corrected with $C_{1s}=285$ eV from contaminant C. The sampling time was 200 ms and the repeat time was 20 for $Ag_{3d5/2}$ peak. For another element the repeat time was 1. The Savitzky method was used in the smoothing. The sample was modified for pellet and set on the sample probe with carbon tape.

Measurements of FT-Raman spectra were performed with Nihon Bunko NR-1800 at room temperature. FT-Raman spectra of the sample powders were measured with Ar ion laser (514.5 nm, 30 mW power) and triple monochrometer. The sample powders were put on the glass plate and arranged plainly its surface with another glass plate.: Ent. slit 500 μm, Sensitivity 1.0 (nA/FS) $\times$ 100, Scan speed of 600 cm^{-1} min^{-1}, Accumulation 3.

3. Results and discussion

3.1. Photochemical property

Fig. 1 shows the absorption spectra of silver-loaded zirconium phosphate [$Ag_xH_{1-x}Zr_2(PO_4)_3$] (3.7 wt.%, 7 wt.%, 11 wt.% Ag content) and no-silver-loaded zirconium phosphate [$HZr_2(PO_4)_3$] water suspensions (0.3 mg cm^{-3}). As shown in Fig. 1, the absorption spectra of the former were different from that of the latter. The absorption of $HZr_2(PO_4)_3$ had no peaks and its absorptivity exponentially decreased from 200 nm to 1000 nm. That of $Ag_xH_{1-x}Zr_2(PO_4)_3$ was broadened and indicated a broad peak at ca. 420

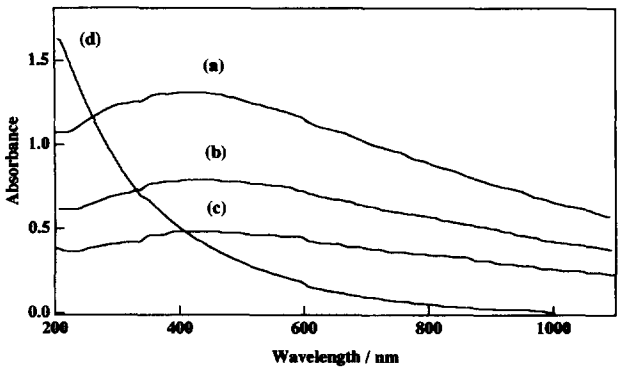

Fig. 1. Absorption spectra of three kinds of silver-loaded zirconium phosphate and no-silver-loaded zirconium phosphate (0.3 mg cm^{-3}) suspensions in water. $Ag_xH_{1-x}Zr_2(PO_4)_3$ (Ag content: (a) 3.7 wt.%, (b) 7 wt.%, (c) 11 wt.%), (d) $HZr_2(PO_4)_3$.

nm in the range of 200 nm to 1100 nm. Since the absorption peak of Ag^+ ion in the $AgNO_3$ aqueous solution was only at ca. 300 nm and that of Ag_3PO_4 was at ca. 494 nm (pale yellow) [10], it seems that Ag^+ ion in $Ag_xH_{1-x}Zr_2(PO_4)_3$ did not form the phosphate compounds and did not elute into the aqueous solution.

Fig. 2a shows the ESR spectrum of DMPO adduct generated by light irradiation of $Ag_xH_{1-x}Zr_2(PO_4)_3$ suspension containing the DMPO spin trap reagent. As shown in Fig. 2a, a typical peak pattern, which each peak height was 1:2:2:1, was observed. From the pattern and their hyperfine splitting constants ($a^N = a_\beta^H = 1.49$ mT), the adduct was assigned to OH radical [11]. Their peaks increased linearly with irradiation time as shown in Fig. 2b and the generation rate of DMPO-OH was calculated to be 0.77 μmol dm^{-3} 20 min^{-1} from the slope shown in Fig. 2. The concentration of DMPO-OH was determined by using the peak area and the concentration of TEMPO as a standard. Therefore, it was found that $OH^\bullet$ was formed by light irradiation of $Ag_xH_{1-x}Zr_2(PO_4)_3$ suspension. DMPO-$O_2^{-\bullet}$ could not be detected in this suspension. Because a reactivity of $OH^\bullet$ with DMPO [$k_{OH} = 3.4 \times 10^9$ (mol $dm^{-3})^{-1}$ s^{-1}] [12] was much larger than that of $O_2^{-\bullet}$ [$k_{O_2^-} = 10$ (mol $dm^{-3})^{-1}$ s^{-1}] [12]. To investigate the contribution of $O_2^{-\bullet}$ for the generation of OH radical, superoxide dismutase, which eliminates $O_2^{-\bullet}$, was added to this system. Addition of SOD to this system gave no change in the peak height of DMPO-OH. Consequently, it seems that this $OH^\bullet$ did not originate from $O_2^{-\bullet}$. Fig. 3 shows the irradiation wavelength dependence for DMPO-OH generation. The generation rate of DMPO-OH adduct increased with a shift of 600 nm to 400 nm light irradiation. The onset wavelength was around 600 nm. The quantum efficiencies at 400 nm and 500 nm were 0.36% and 0.037%, respectively. On the other hand, when I^- ion as a scavenger of $OH^\bullet$ was added to the suspension and irradiated, the signal of DMPO-OH disappeared and the different signal pattern was observed. This indicates the interaction between $OH^\bullet$ and I^- ion. ($OH^\bullet + I^- \rightarrow 1/2I_2 + OH^-$; $k = 1.1 \times 10^{10}$ (mol $dm^{-3})^{-1}$ s^{-1}) [13]. Addition of SOD to this suspension

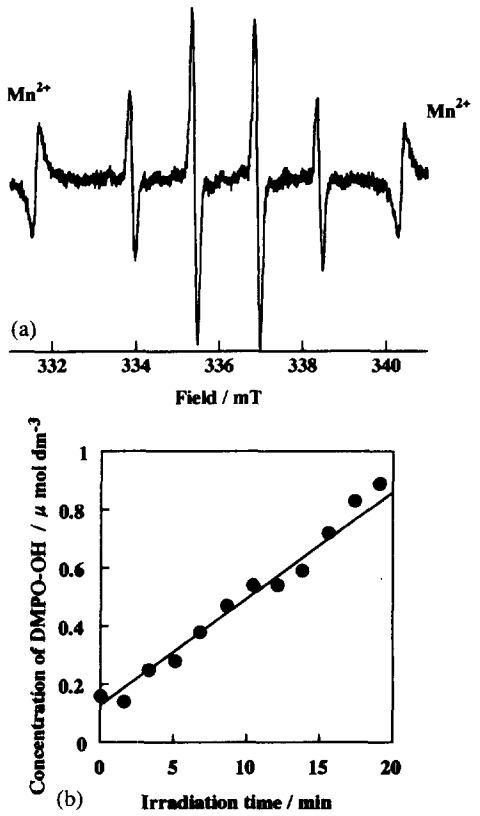

Fig. 2. ESR spectrum of DMPO-OH generated in the irradiated $Ag_xH_{1-x}Zr_2(PO_4)_3$ water suspension. Hyperfine splitting correspond to $a^N = a^H = 1.49$ mT, $Ag_xH_{1-x}Zr_2(PO_4)_3$ (11 wt.% Ag content) suspension in aqueous solution: 0.95 mg cm^{-3} (contained 0.43 mol dm^{-3} DMPO). Light source: 500 W Xe lamp (KL-50 Interference and UV-37 cut-off filters) Recorded Power: 8 mW, Mod. Width: 79 μT, Accumulation times: 5 s × 12. (b) Plot of generation rate of DMPO-OH vs. irradiation time. $Ag_xH_{1-x}Zr_2(PO_4)_3$ (11 wt.% Ag content) suspension in pH 5.8 phosphate buffer solution: 0.95 mg cm^{-3} (contained 0.43 mol dm^{-3} DMPO). Light source: 500 W Xe lamp (KL-50 Interference and UV-37 cut-off filters) Recorded Power: 8 mW, Mod. Width: 79 μT, Accumulation times: 5 s × 12.

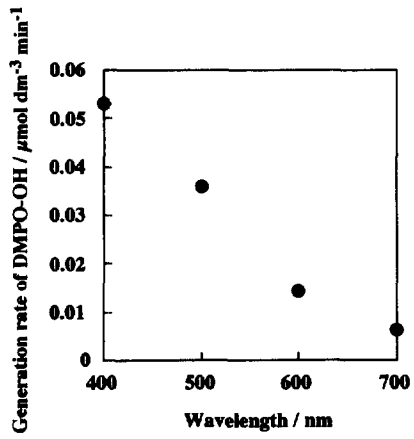

Fig. 3. Plot of generation rate of DMPO-OH vs. irradiation wavelength. The experimental conditions were the same as those of Fig. 2a. Light source: 500 W Xe lamp (KL-40, KL-50, KL-60, KL-70 Interference filters and UV-37, Y-48, O-58 cut-off filters, respectively). The quantum efficiencies at 400 nm and 500 nm were 0.36% and 0.037%, respectively.

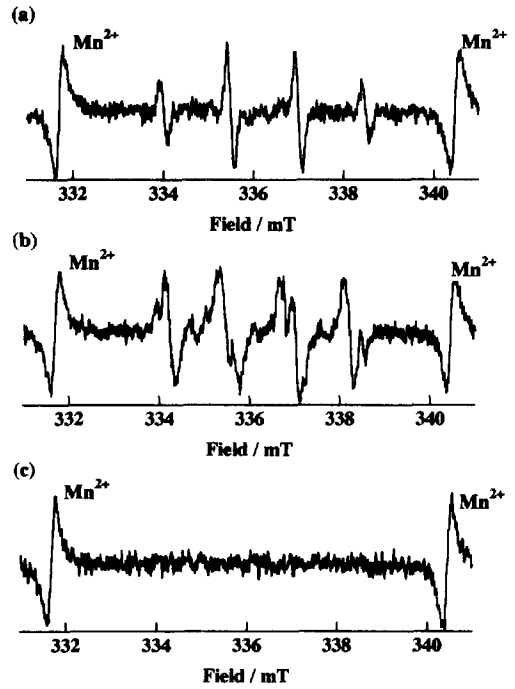

Fig. 4. ESR spectra of DMPO-OH adducts observed in irradiated $Ag_xH_{1-x}Zr_2(PO_4)_3$ (11 wt.% Ag content) suspensions with adding of no ion (a), I^- ion (b), and SOD (c) $Ag_xH_{1-x}Zr_2(PO_4)_3$ suspension: (a) 0.89 mg cm^{-3} (contained 0.43 mol dm^{-3} DMPO), (b) 0.89 mg cm^{-3} (contained 0.43 mol dm^{-3} DMPO and 0.1 mmol dm^{-3} I^-), (c) 0.83 mg cm^{-3} (contained 0.43 mol dm^{-3} DMPO and 13.5 unit SOD 0.02 cm^3). Light source: 500 W Xe lamp (KL-40 Interference and UV-37 cut-off filters), Irradiation time: 21 min Recorded Power: 8 mW, Mod. Width: 79 μT, Accumulation times: 5 s × 12.

eliminated that signal as shown in Fig. 4. These indicate that $O_2^{-\cdot}$ could be observed in the presence of I^- ion as a $OH^\cdot$ scavenger in this water suspension. Therefore, in $Ag_xH_{1-x}Zr_2(PO_4)_3$ water suspension a reaction scheme on light-induced generation of $O_2^{-\cdot}$ and $OH^\cdot$ was proposed as follows.

$$Ag_xH_{1-x}Zr_2(PO_4)_3 + h\nu \rightarrow Ag_xH_{1-x}Zr_2(PO_4)_3\ (e^- \text{ and } h^+) \quad (1)$$

$$e^- + O_2 \rightarrow O_2^{-\cdot} \quad (2)$$

$$O_2^{-\cdot} + DMPO \rightarrow DMPO\text{-}O_2^- \quad (3)$$

(in the presence of I^- ion as a $OH^\cdot$ scavenger)

$$h^+ + OH^- \rightarrow OH^\cdot \quad (4)$$

$$OH^\cdot + DMPO \rightarrow DMPO\text{-}OH \quad (5)$$

The generation rate of DMPO-OH increased with Ag content as shown in Table 1. No-silver-loaded zirconium phosphate also indicated the small generation of DMPO-OH. Therefore, it seems that the zirconium phosphate has a property of oxidizing OH^- ion. Consequently, a more consideration about the part of Eq. (1) will be needed. The dependence of irradiation wavelength for the generation rate of DMPO-OH was similar to the absorption spectrum of $NH_4Zr_2(PO_4)_3$, not for $Ag_xH_{1-x}Zr_2(PO_4)_3$ as shown in Fig. 3. This wavelength dependence indicates that by excited $HZr_2(PO_4)_3$ crystal the charge separation would occur. If the charge separation occurred on the irradiated $HZr_2(PO_4)_3$ crystal, the photocurrent would be observed. The $HZr_2(PO_4)_3$ modified electrode was prepared for the photoelectrochemical measurement. $HZr_2(PO_4)_3$ powder as the no-silver-loaded zirconium phosphate and Nafion alcohol solution were mixed and coated on Pt electrode. Such prepared $HZr_2(PO_4)_3$/Nafion modified electrode was stable in the aqueous solution. Light irradiation was performed with 500 W superhigh pressure mercury lamp (UV-35 cut off filter). Fig. 5 shows the relation between photocurrent and irradiation time. Irradiation of $HZr_2(PO_4)_3$/Nafion modified Pt electrode at −0.2 V vs. SCE in 0.1 M Na_2SO_4 aqueous solution caused the generation of photocurrent. As shown in Fig. 5, 26.1 μA cm^{-2} of the photocathodic current was observed under irradiation. This indicates that the electron from Pt electrode transferred to the positive hole generated on $HZr_2(PO_4)_3$ by light irradiation. Consequently, the charge separation was certificated and $HZr_2(PO_4)_3$ would have the property of a semiconductor. Then the role of Ag^+ ion in the photogeneration of superoxide radicals would be needed in the discussion.

3.2. Surface characterization

The relation between the surface atomic ratio of Ag and the generation rate of DMPO-OH was investigated by XPS technique. Table 1 shows the generation rate of DMPO-OH

Table 1
Binding energies, the atomic ratio of surface region determined by XPS, and generation rate of DMPO-OH

	$Ag_{3d5/2}$ (eV)	O_{1S} (eV)	P_{2p} (eV)	$Zr_{3s1/2}$ (eV)	Ag/P	Zr/P	Ag/Zr	DMPO-OH [a] (μmol dm^{-3} 20 min^{-1})
3.7 wt.%	368.9	532.1	134	434	0.025	0.29	0.087	0.27
7 wt.%	369.1	532	134.2	434	0.063	0.5	0.13	0.65
11 wt.%	368.8	532	133.8	434.5	0.086	0.38	0.23	0.76
no Ag	–	532	134	434.3	–	0.41	–	0.14

[a] Light source: 500 W Xe lamp with 500 nm interference and UV-37 filters $Ag_xH_{1-x}Zr_2(PO_4)_3$ (11 wt.% Ag content) or $NH_4Zr_2(PO_4)_3$ suspension in pH 5.8 phosphate buffer solution: 0.95 mg cm^{-3} (contained 0.43 mol dm^{-3} DMPO).

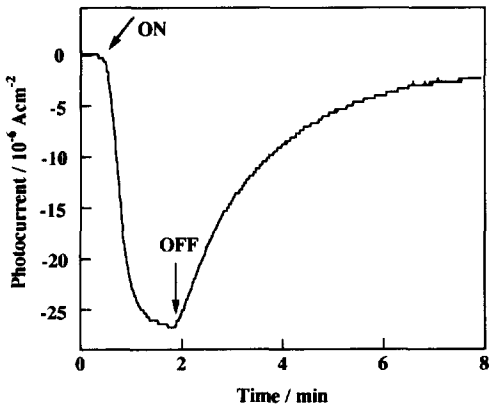

Fig. 5. Transient photocurrent behavior at a Pt electrode at −0.2 V vs. SCE, induced by illumination of $HZr_2(PO_4)_3$/Nafion in 0.1 mol dm^{-3} Na_2SO_4. The amount of the coated $HZr_2(PO_4)_3$ was 32 μg cm^{-2}. Light source: 500 W super high pressure mercury lamp (UV-35 cut-off filter).

and the atomic ratio of Ag/P, Zr/P, and Ag/Zr on the surface of $Ag_xH_{1-x}Zr_2(PO_4)_3$ powder. Those atomic ratios were calculated from each peak area of $Ag_{3d5/2}$, P_{2p}, $Zr_{3s1/2}$ in XPS spectra. The obtained binding energy of these $Ag_{3d5/2}$ peaks were the almost same values and they did not change with Ag content. It is reported that the binding energy of $Ag_{3d5/2}$ (metal) is 368.22 eV [14] and that of Ag_2O is 367.8 eV [15]. The values observed for $Ag_xH_{1-x}Zr_2(PO_4)_3$, i.e., 368.8 eV (Ag 3.7 wt.%), 368.9 eV (Ag 7 wt.%), and 369.1 eV (Ag 11 wt.%), were larger than that of Ag metal and were different from that of Ag_2O. Since Na atoms in $NaZr_2(PO_4)_3$ are octahedrally surrounded by oxygen atom (O_3ZrO_3-NaO_3ZrO_3), Ag atoms in $Ag_xH_{1-x}Zr_2(PO_4)_3$ would also be in the same position [16]. Therefore, Ag^+ ion would be stabilized by the surrounded oxygen atoms. The electron density of Ag^+ ion would become larger than that of free Ag^+ ion by the $-I$ effects of the surrounded oxygen atoms. We indicate such Ag^+ ion as $Ag_{surface}{}^+$. Binding energies of O_{1s}, P_{2p}, and $Zr_{3s1/2}$ were the same values as that of no Ag sample. Loading of silver to zirconium phosphate did not change the electronic state of the constituted ions on the surface. As shown in Table 1, when the ratios of Ag to Zr and P on the surface were increased, the generation rate of DMPO-OH was increased. Matsuoka et al. reported that Ag^+ ion in Ag^+/ZSM-5 catalyst was excited by the wavelength of 200 nm to 250 nm [6]. Since it seems that Ag^+ ion on the surface of $Ag_xH_{1-x}Zr_2(PO_4)_3$ could not be directly excited by Xe lamp irradiation in the wavelength range of 400 nm to 600 nm, $Ag_{surface}{}^+$ would be related to the charge separation on the photoirradiated $HZr_2(PO_4)_3$. When $HZr_2(PO_4)_3$ was irradiated, $Ag_{surface}{}^+$ would work as an electron pool [17] and O_2 molecule adsorbed on this site would be reduced to $O_2^{-\bullet}$. Thus, the charge separation occurred effectively.

$$HZr_2(PO_4)_3 + h\nu \rightarrow HZr_2(PO_4)_3\ (e^- \text{ and } h^+) \quad (6)$$

$$e^- + (Ag^+_{surface})\text{-}O_2 \rightarrow (Ag^0_{surface})\text{-}O_2 \rightarrow O_2^{-\bullet} + Ag^+_{surface} \quad (7)$$

(electron pool)

$$h^+ + OH^- \rightarrow OH^\bullet \quad (8)$$

Since $Ag_xH_{1-x}Zr_2(PO_4)_3$ suspension did not color during light irradiation, the removal rate of electron by O_2 molecule in the reaction of Eq. (7) seems to be fast. However, when the high intensity light irradiation such as 500 W superhigh pressure mercury lamp without cut-off filter was irradiated to the $Ag_xH_{1-x}Zr_2(PO_4)_3$, the suspension's color became black under air. In this case, the generation rate of electron would be faster than the removal rate of it from $Ag_{surface}{}^0$ site. O_2 molecules as an electron acceptor is known to adsorb on Ag due to interaction between them. O_2 adsorption to Ag metal and its interaction between O_2 and Ag have been already reported in detail. Adsorption of O_2 molecule to $Ag_xH_{1-x}Zr_2(PO_4)_3$ powder was investigated by measurement of FT-Raman spectra. FT-Raman spectra of $Ag_xH_{1-x}Zr_2(PO_4)_3$ and no-silver-loaded sample powders are shown in Fig. 6. With increase of Ag content some new peaks, that is, ca. 191 cm^{-1}, 328 cm^{-1}, 427 cm^{-1}, and 1033 cm^{-1}, appeared. The peaks except for them were agreed with those of zirconium phosphate as shown in Fig. 6. Those peaks were different from both the peaks in 700 cm^{-1} to 500 cm^{-1} of Ag_2O and the intense peak at 432 cm^{-1}, weak peak at 469 cm^{-1}, 493 cm^{-1} of AgO [18]. These indicate that such Ag_2O and AgO was not formed on the surface. For Ag/ZrO_2 240 cm^{-1} and 345 cm^{-1} of Raman shift [19] are attributed to Ag–O and Ag–O_2 vibrational frequencies, for Ag/SiO_2 995 cm^{-1} of Raman shift are due to Ag–O_2^- [19]. Consequently, the new peaks at 191 cm^{-1}, 328 cm^{-1}, and 1033 cm^{-1} seems to be due to $Ag_{surface}{}^+$–O and $Ag_{surface}{}^+$–O_2 vibrational frequencies. Though the peak at 427 cm^{-1} could not be assigned with the above vibrational frequency, it would be also related with the interaction between $Ag_{surface}{}^+$ and oxygen atoms.

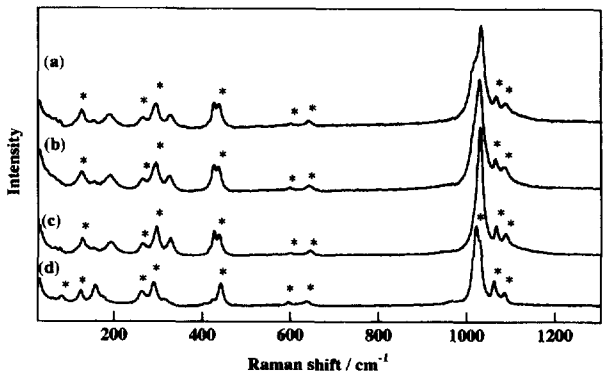

Fig. 6. FT-Raman spectra of $Ag_xH_{1-x}Zr_2(PO_4)_3$ and $NH_4Zr_2(PO_4)_3$ powders. (a) 11 wt.% Ag content, (b) 7 wt.% Ag content, (c) 3.7 wt.% Ag content, (d) 0 wt.% Ag content, *corresponds to some peaks of $NH_4Zr_2(PO_4)_3$ powder. Light source: Ar ion laser (λ_{ex} = 514.5 nm, 30 mW power), Ent. slit 500 μm, Sensitivity 1.0 (nA/FS) × 100, Scan speed 600 cm^{-1} min^{-1}, Accumulation times: 3.

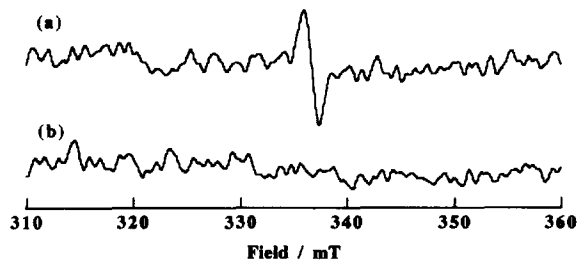

Fig. 7. ESR spectra of $Ag_xH_{1-x}Zr_2(PO_4)_3$ powder (11 wt.% Ag content) in vacuo (a) and in the air (b) at room temperature. $Ag_xH_{1-x}Zr_2(PO_4)_3$ powder: 60 mg Recorded power: 1 mW, Mod. Width: 0.25 mT, Accumulation times: 5 s × 120.

Because it appeared by loading Ag^+ ion to zirconium phosphate. The differences of Raman shifts would be due to the difference between the electronic state of $Ag_{surface}{}^+$, which indicated by the binding energy of $Ag_{3d5/2}$ peak, and that of Ag^0. These data indicate that the $Ag_{surface}{}^+$ behaves similarly as the Ag^0 or Ag cluster. Fig. 7 shows the ESR spectra which are due to the interaction between O_2 molecule and silver-loaded zirconium phosphate. ESR spectra of three kinds of $Ag_xH_{1-x}Zr_2(PO_4)_3$ powders (Ag content: 3.7 wt.%, 7 wt.%, 11 wt.%) indicated one peak at $g = 2.0036$ at room temperature and 77 K in vacuo, but not observed for $HZr_2(PO_4)_3$ and $AgNO_3$. The peak disappeared on exposure to air. And it was decreased to about 25% by heating at 423 K. Li and Vannice have reported one peak at $g = 2.0028$ in Ag/SiO_2 [5]. They were assigned with conduction electrons existing in small silver nanocrystallites. And the adsorption of O_2 to the small silver nanocrystallites at either 300 or 443 K leaded the decrease of intensity. It was concluded that the chemisorbed oxygen atoms strongly interact with the conduction electrons to form essentially surface O^{2-} type species. Therefore, it was found that the peak observed for silver-loaded hydrogen zirconium phosphate is similar to that in Ag/SiO_2. The observed peak seemed to be due to the conduction electrons of $Ag_{surface}{}^+$, which was formed by the $-I$ effects of the surrounded oxygen atoms.

4. Conclusions

Loading of Ag^+ ion to zirconium phosphate lead to the generation of the $Ag_{surface}{}^+$ site which was formed by the $-I$ effects of the surrounded oxygen atoms and had a conduction electron. It was found that such site interacts with the adsorbed oxygen molecules and form $Ag_{surface}{}^+$–O^{2-} type species on the surface. In the irradiation to zirconium phosphate modified Pt electrode a photocathodic current was observed and a charge separation on zirconium phosphate was indicated. Therefore, it was found that such $Ag_{surface}{}^+$ worked as an electron pool during irradiation.: When the charge separation occurs on the irradiated $HZr_2(PO_4)_3$, the photogenerated electron transfers to the O_2 molecule via the $Ag_{surface}{}^+$ site as the electron pool and $O_2{}^-$ radical generates. The photogenerated positive hole oxidizes OH^- ion in water and generates the OH radical.

Acknowledgements

We thank Toa Gousei in Japan for support of the zirconium phosphate samples and silver-loaded ones used in this work. FT-Raman spectra were measured at the Center for Cooperative Research in Tokushima University. We also thank Dr. Shigeru Sugiyama for ESCA measurement and useful discussion.

References

[1] A. Henglein, J. Phys. Chem. 83 (1979) 2209.
[2] A. Henglein, J. Am. Chem. Soc. 103 (1981) 1059.
[3] T. Sun, K. Seff, Chem. Rev. 94 (1994) 858.
[4] J. Michalik, H. Yamada, D.R. Brown, L. Kevan, J. Phys. Chem. 100 (1996) 4213.
[5] X. Li, A. Vannice, J. Catal. 151 (1995) 87.
[6] M. Matsuoka, E. Matsuda, K. Tsuji, H. Yamashita, M. Anpo, J. Mol. Catal., A: Chemical 107 (1996) 399.
[7] H. Kourai, K. Nakagawa, Y. Yamada, J. Antibact. Antifung. Agents Jpn. 21 (1993) 77.
[8] H. Kourai, Y. Manabe, Y. Yamada, J. Antibact. Antifung. Agents Jpn. 22 (1994) 595.
[9] J.B. Goodenough, H.Y.P. Hong, J.A. Kafalas, Mater. Res. Bull. 11 (1976) 203.
[10] K. Tennakone, A.H. Jayatissa, W. Wijeratne, J. Chem. Soc., Chem. Commun. (1988) 496.
[11] E. Finkelstein, G.M. Rosen, E.J. Rauckman, J. Am. Chem. Soc. 102 (1980) 4994.
[12] E. Finkelstein, G.M. Rosen, E.J. Rauckman, Arch. Biochem. Biophys. 177 (1980) 1.
[13] G.V. Buxton, C.L. Greenstock, W.P. Helman, A.B. Ross, J. Phys. Chem. Ref. Data 17 (1988) 513.
[14] R. Nyholm, N. Martensson, Solid State Commun. 40 (1981) 311.
[15] S.W. Gaarenstroom, N. Winograd, J. Chem. Phys. 67 (1977) 3500.
[16] L.O. Hangman, P. Kierkegaard, Acta Chem. Scand. 22 (1968) 1822.
[17] A. Henglein, J. Phys. Chem. 83 (1979) 2209.
[18] M. Kilo, C. Schild, A. Wokaun, A. Baiker, J. Chem. Soc., Faraday Trans. 88 (1992) 1453.
[19] D.I. Kondarides, G.N. Papatheodorou, C.G. Vayenas, X.E. Verykios, Ber. Bunsenges. Phys. Chem. 97 (1993) 709.